Silencing tankyrase and telomerase promotes A549 human lung adenocarcinoma cell apoptosis and inhibits proliferation

HONGDA LU[1,2], ZHANG LEI[1,2], ZHONGXIN LU[2], QIANMING LU[1,2], CHI LU[1,2], WEIQUN CHEN[2], CHUN WANG[1], QIU TANG[1] and QINGZHI KONG[1,2]

[1]Department of Oncology, the Central Hospital of Wuhan;
[2]Cancer Research Institute of Wuhan, Wuhan, Hubei, P.R. China

Received June 17, 2013; Accepted July 30, 2013

DOI: 10.3892/or.2013.2665

Abstract. Telomeres are the end structures of chromosomes in mammalian cells; they play a pivotal role in maintaining the stability of the chromosome and become shorter with each cell division. However, several types of tumor cells express telomerase in very high levels to overcome this crisis and achieve the ability to proliferate endlessly. The telomerase inhibitors can partly inhibit tumor cell proliferation and promote apoptosis, but their roles are only limited. Tankyrase is a poly(ADP-ribose) polymerase which has synergistic effect on telomerase, and is expressed in lung cancer cells in high levels. In the present study, antisense oligonucleotides of telomerase (ashTERT) and tankyrase (asTANKS) were used as specific inhibitors to silence the expression of target genes in A549 human lung adenocarcinoma cells by transfection. The results showed that ashTERT and asTANKS suppressed the expression of telomerase and tankyrase significantly; both inhibited the activity of telomerase and the combination group achieved better effect, but only ashTERT shortened the length of telomeres, asTANKS did not. Further studies showed that ashTERT and asTANKS-promoted A549 apoptosis was not mediated by downregulation of the expression of the anti-apoptotic gene BCL-2 or upregulation of the expression of the pro-apoptotic gene BAX, but by adjusting the two isoforms proportion of myeloid cell leukemia-1 (MCL-1) which can interact with tankyrase directly. MCL-1short (MCL-1S), a pro-apoptotic gene, increased more than MCL-1Long (MCL-1L) which is an anti-apoptotic gene, leading to A549 cell apoptosis and a similar result was obtained in nude mice *in vivo*. The present study suggests that combination of the inhibitors of telomerase and tankyrase can be used as a strategy for the treatment of lung cancer in humans.

Correspondence to: Professor Qingzhi Kong, Department of Oncology, the Central Hospital of Wuhan, 26 Shengli Street, Jianghan Road, Wuhan, Hubei 430014, P.R. China
E-mail: phlonda@163.com

Key words: tankyrase, telomerase, antisense oligonucleotide, apoptosis, proliferation, lung adenocarcinoma A549 cells

Introduction

Lung cancer is a malignant tumor with some of the highest incidence and mortality rates worldwide; moreover, for most patients, radical cure operation is not an option when the symptoms appear and the disease is found, therefore, their prognosis is very poor (1). The efficiency of chemotherapy and radiotherapy is low and the considerable side-effects are too strong for some patients to endure (2). With the advancements in the research, a significant number of drugs against lung cancer are being developed and although considerable achievements have been made, a lot remains to be studied in order to control lung cancer.

Telomeres, the end of eukaryote linear chromosomes consisting of tandem arrays of telomeric repeats, protect the genome from degradation. In somatic cells, telomeres shorten with each cell division due to the 'end-replication-problem'. Critically short telomeres induce an irreversible exit from the cell cycle, known as senescence (3). Thus, telomere loss is considered as a 'mitotic clock' that limits the proliferation capacity of somatic cells. However, in immortal cells, including tumor cells, telomerase provides a means to replace telomere repeats which are lost during replication as a result of the inability of DNA polymerase to replicate to the end of linear chromosomes. Telomerase activity not only maintains the telomeres of proliferating cells but is implicated in the process of cellular immortalization and oncogenesis (4). In particular, tumor cells with positive expression of telomerase have undergone senescence and have obtained a considerable ability to proliferate.

Inhibition of telomerase has been discussed as a promising approach for treating a variety of malignant tumors, as the prerequisites agreed that telomerase was the main mechanism of telomere maintenance (5). However, it was independent of (uncoupled from) the proliferation of tumor cells even if telomerase activity is diminished. In other words, there is a lag phase between the times telomerase is inhibited and when telomeres shorten sufficiently to cause cellular crisis with proliferation strangled, and no host can suffer from so much neoplastic burden so many times (6).

In this case, another factors of regulator for telomere maintenance, tankyrase was advert, which poly (ADP-ribosyl) ate telomere-repeat-binding factor 1 (TRF1) and releases it from

telomeres, allowing access of telomerase to telomeres and enhancing telomere elongation. Conversely, it was possible that the combination of both enzyme inhibitors can increase the risk of critically shortened telomere and promote the following crisis and mortality of lung cancer cells (7).

Materials and methods

Mice and cell lines. BALB/c nude mice, 6-8 weeks old, were purchased from the Center of Medical Experimental Animals of Hubei Province (Wuhan, China). The animals were housed and used for studies approved by the Animal Care and Use Committee of the central hospital of Wuhan. A549 human lung adenocarcinoma cell lines were obtained from the China Center for Type Culture Collection (CCTCC) in Wuhan University, China. After thawing, cells were transferred into culture flasks containing RPMI-1640 (Gibco) supplemented with 1% penicillin-streptomycin and 10% fetal bovine serum (FBS), and propagated in a humidified 5% CO_2 incubator at 37˚C. The exponentially growing cells were harvested when reaching 80-90% confluence.

Oligonucleotide synthesis and preparation of reagents. An optimal target is a 25-base sequence that lies within the region from the 5'-cap through the first 25 bases of coding sequence, has ~50% GC content and has little or no secondary structure (7). All oligonucleotides in these experiments were designed by a computational neural network. BLAST confirmed they are specific for their mRNA (http://www.ncbi.nlm.nih.gov/BLAST/). The oligonucleotides were synthesized by Sangon Biotechnology Engineering Company of Shanghai, China, including antisense oligonucleotides for human telomerase reverse transcriptase (ashTERT) and tankyrase (asTANKS), and corresponding sense oligonucleotides for human telomerase reverse transcriptase (shTERT) and tankyrase (sTANKS) used as control as well. The sequences of oligonucleotides were: ashTERT, 5'-GGAGCGCGCGGCATCGCGGG-3'; asTANKS, 5'-CATCTTCGGACTCCCCTAGCACTG-3'; shTERT, 5'-CCCGCGATGCCGCGCGCTCC-3'; sTANKS, 5'-CAGTGCTAGGGGAGTCCGAAGATG-3'. The synthesized oligonucleotides were modified by phosphorothiolation, purified by HPLC, stored at -20˚C.

Oligofectamin Reagent (Invitrogen) was applied in order to improve oligonucleotide merging with cell membrane. RNA TRIzol Reagent was obtained from Invitrogen, First Strand cDNA Synthesis Reagent was purchased from Gibco, TRAPeze ELISA Telomerase Detection kit was obtained from Millipore, Telomere PNA kit was provided by Dako and Quantum premixed fluorescein isothiocyanate (FITC) MESF beads were purchased by Flow Cytometry Standards Co.

Transfection of oligonucleotides. Owing to different oligonucleotides, A549 cells were divided into 6 groups: shTERT, ashTERT, ashTERT plus asTANKS, asTANKS, sTANKS and blank control, and the concentration applied was 2 μM. Oligofectamin concentration depended on oligonucleotide dose according to the manufacturer's protocol. Briefly, cells were plated into 96-well plates and incubated until the cells reached 30-50% confluence. Before transfection, oligonucleotides drug were diluted with serum-free medium. Then, the desired amount of oligonucleotide was incubated for 15-20 min with diluted Oligofectamin. The oligonucleotide/Oligofectamin mixture (20 μl) was added drop-wise in 80 μl RPMI-1640. After co-incubating for 48 h at 37˚C, 50 μl RPMI-1640 containing 5% FBS was added into each well instead of drugs and cells were analyzed respectively.

RT-PCR assay. The expression of hTERT mRNA was detected by RT-PCR assay. Total cellular mRNA was isolated with TRIzol Reagent. RNA sample was quantitated by measurement of optic absorbance (A) at 260/280 nm in a spectrophotometer and the rate of A260/A280 ranged between 1.8-2.0. Two micrograms of total RNA were reverse transcribed into cDNA in a volume of 20 μl by Reverse Transcription kit using M-MuLV reverse transcriptase and oligo (dT) 18 primer (MDI Fermentas). The mixture was incubated at 42˚C for 60 min and heated to 70˚C for 10 min to stop reaction. PCR was performed on a DNA thermal cycler with primers (Sangon Biotechnology Engineering Company of Shanghai, China) specific for hTERT, tankyrase, B-cell CLL/lymphoma 2 (BCL-2), BAX, myeloid cell leukemia-1 (MCL-1) and β-actin; all the sequences were blasted (http://www.ncbi.nlm.nih.gov/BLAST/). The primers were: hTERT (263 bp) forward, 5'-TGCGTTTGGTGGATGATTTCTTGT-3' and reverse, 5'-CCGGGCATAGCTGGAGTAGTCG-3'; tankyrase (763 bp) forward, 5'-GGGCGGAAAGACGTAGTTGA-3' and reverse, 5'-TTAACTGTGGTGTGGGAGCC-3'; BCL-2 (708 bp) forward, 5'-CGGAATTCTATGGCGCAAGCCGGGAG-3' and reverse, 5'-CGGTACCTCACTTGTGGCCCAGGTATGCACC-3'; BAX (360 bp) forward, 5'-AAGCTGAGCGAGTGTCTCCGGCG-3' and reverse, 5'-GCCACAAAGATGGTCACTGTCTGCC-3'; MCL-1 (970 bp) forward, 5'-CGGTAATCGGACTCAACCTCT-3' and reverse, 5'-ACATTCCTGATGCCACCTCTA-3'; β-actin (541 bp) forward, 5'-GTGGGGCGCCCCAGGCACCA-3' and reverse, 5'-CTCCTTAATGTCACGCACGATTTC-3'. Reverse transcription product (cDNA) (2 μl) was added to the PCR mixture (Takara Co.) for amplification in a volume of 50 μl. The amplification profile was: 94˚C 45 sec, 57-62˚C 55 sec, 72˚C 60 sec, 32 cycles, finally 72˚C 10 min. The products amplified were subjected to 2% agarose gel electrophoresis and bands were visualized by staining with ethidium bromide and images were captured under ultraviolet lamp.

Polymerase chain reaction enzyme-linked immunosorbent assay (PCR-ELISA). PCR-ELISA assay was measured according to the manufacturer's protocol of TRAPeze ELISA Telomerase Detection kit (Invitrogen) with a minor modification. Cultured A549 cells were harvested at a density of $1x10^5$/well and washed with PBS, then homogenized in 200 μl CHAPS lysis buffer and left on ice for 20 min, and 60 μl of supernatant was collected after centrifugation (12,000 x g, 20 min, 4˚C). PCR was performed in 50 μl supernatant containing 10 μl transfer reaction mixture, 2 μl of cell extracts was added to 23 μl of nuclease-free water. The PCR conditions were: the telomerase reaction was carried out at 25˚C for 10 min, followed by a two-step PCR amplification (94˚C 40 sec, 50˚C 40 sec, 72˚C 90 sec, 33 cycles). After equilibrating at 72˚C for 10 min, 5 μl amplified product and 20 μl denatured reagent were incubated at room temperature. Hybridization buffer (225 μl) was then added and mixed, and 100 μl of

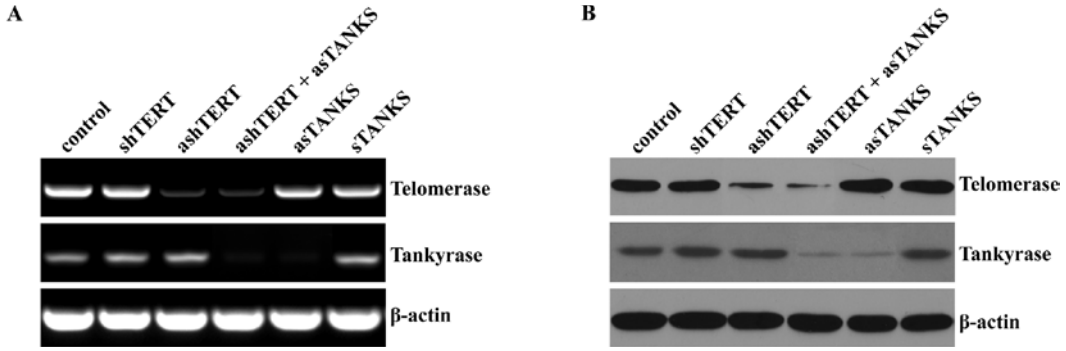

Figure 1. The expression of telomerase reverse transcriptase, tankyrase and β-actin in A549 cells. A549 cells were transfected with ashTERT or asTANKS and the corresponding sense control oligonucleotide respectively; 48 h later, the expression of telomerase, tankyrase and β-actin were detected by (A) RT-PCR and (B) western blotting. The results showed that ashTERT and asTANKS decreased telomerase and tankyrase expression in both the mRNA and the protein level.

anti-DIG-POD working solution was added and incubated for another 30 min followed by the addition of 100 μl TMB substrate solution and 100 μl of stop reagent was added. The absorbance in each well was read at the wavelength of 450 and 690 nm by microtiter plate reader and the value for each sample was computed as $A_{sample} = A_{450nm} - A_{690nm}$. TSR8 with 8 telomeric repeats was used as PCR-ELISA positive control (the range of $A_{450nm} - A_{690nm}$ must be >0.8), and CHAPS lysis buffer without tissue extract and heat-treated (80˚C, 20 min) as negative control (the range of $A_{450nm} - A_{690nm}$ must be < 0.25). The net increased rate of absorbance for the sample was recorded as $\Delta A\ (\%) = (A_{sample} - A_{negative})/(A_{positive} - A_{negative}) \times 100\%$.

Q-FISH assay. Briefly, FACSCalibur System (BD Biosciences) was calibrated by MESF Quantum 24 Fluorescent Beads and slope calculated on account of the linear relationship between the MESF beads and fluorescent channel. According to the manufacturer's protocol for the Telomere PNA kit for Flow Cytometry (Dako), hybridization was performed in 300 μl buffer solution PNA probe at 0.3 μg/ml containing pellet centrifuged from $5x10^5$ washed A549 cells. After incubating at 82˚C for 20 min and mixed by vortexing 2 h in the dark, resuspended cells were collected in 1 ml wash buffer, mixed and incubated in a 40˚C water bath for 10 min. Centrifuged cells (500 x g, 7 min) were added to 500 μl of DNA staining buffer, transferred to standard polystyrene flow cytometry tubes and incubated at room temperature for 2 h. As the same installation as that used for the MESF beads, samples were detected and G_0/G_1 cells were gated from the scatter plot forward scatter (FSC) vs. DNA dye fluorescence with linear scaling. FITC fluorescence was displayed on histogram gated on the population, while mean fluorescence intensity (MFI) was recorded and buffer without cell sample blank control as well. The mean telomere length was calculated as: $TL\ (kb) = (MFI_{sample} - MFI_{blank}) \times 0.019 \times 0.02604/sec$.

Western blotting. A549 cells ($5x10^5$) were rinsed with ice-cold PBS, agitated constantly at 4˚C for 30 min followed by centrifugation with RIPA buffer (12,000 x g, 20 min). The supernatant was aspirated and the protein concentration levels were detected by a Bradford assay, which determined whether samples were fit for test as followed. Through denaturation by anionic detergent sodium dodecyl sulfate (SDS), 20 μg samples were loaded to 8% polyacrylamide gel and β-actin as positive control. SDS-polyacrylamide gel electrophoresis (PAGE) was carried out and protein blotting was transferred to PVDF membranes, in which transferred efficiency was checked by ponceau staining soon after. Membranes were blocked for 2 h at room temperature in 10% blocking buffer and incubated overnight with first antibody at 4˚C, followed by peroxidase-conjugated secondary lgG. Finally, chemiluminescence emanating from membranes was revealed and images were captured. The first antibodies of β-actin, MCL-1, BCL-2 and BAX were purchased from Santa Cruz and the first antibodies of telomerase and tankyrase were purchased from Abcam; all the peroxidase-conjugated second antibodies were purchased from EarthOx.

Apoptosis assay. Apoptosis was detected by flow cytometry using Annexin V Apoptosis Detection kit FITC (eBioscience). A549 cells transfected with or without oligonucleotide were harvested 48 h later. After washing cells once with binding buffer, cells were stained by Apoptosis Detection kit according to the manufacturer's instructions. The samples were tested by FACSCalibur System (Becton-Dickinson) and the data were analyzed with FlowJo (v7.6.5) software.

Hoechst 33342 staining. A549 cells were plated in 6-well plates and were fixed with 4% paraformaldehyde for 10 min at 25˚C and cells were washed twice in PBS. Hoechst 33342 staining (1 mM; Sigma-Aldrich) solution was added to the plate and incubated for 15 min in the dark at 37˚C; the staining solution was discarded and washed twice in PBS. Stained cells were observed by fluorescence microscopy (Olympus).

MTT assay. A549 cells were seeded in 96-well plates at a density of 2,000 cells/well containing 200 μl RPMI-1640 medium and transfected with oligonucleotide. Forty-eight hours later, 20 μl of MTT (5 mg/ml; Sigma-Aldrich) was added to each well and incubated for 4 h at 37˚C avoiding light. The medium was removed and the formazan was dissolved in 150 μl of DMSO. Absorbance was measured at 490 nm. Cell inhibition rate was calculated as $\%\ IR = (1 - OD_{experiment}/OD_{control}) \times 100\%$.

Cell proliferation assay. A549 cells ($1x10^6$) were suspended in 1 ml RPMI-1640 without FBS, 1 μl of 5 mM carboxyfluorescein diacetate succinimidyl ester (CFSE; Molecular Probes) was added in the tube. The cells were place at 37˚C for 10 min away from light; then, 5 volumes FBS was added and mixed,

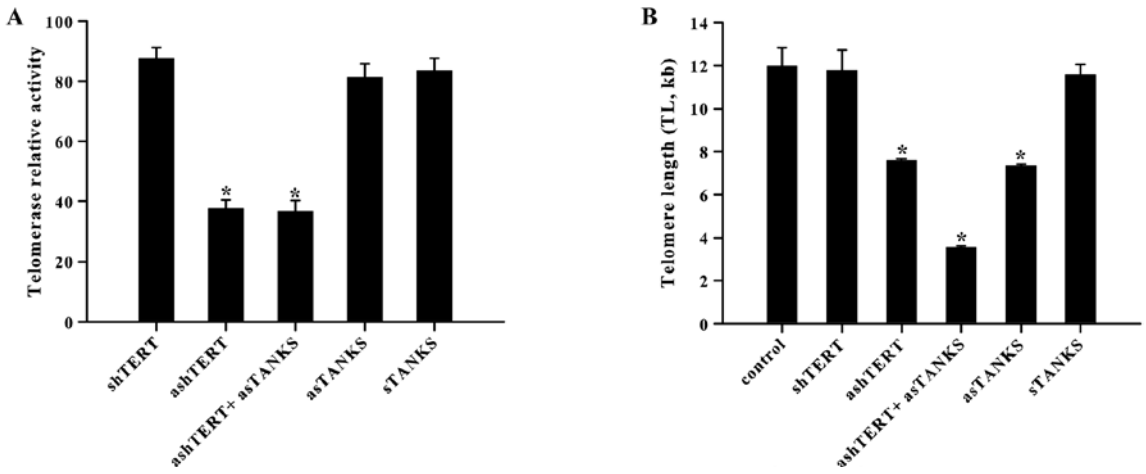

Figure 2. The telomerase relative activity and telomere length in A549 cells. (A) Forty-eight hours after transfection, the supernatant of A549 cell lysis was collected and the telomerase relative activity was detected by PCR-ELISA assay. (B) Telomere length of transfected A549 cells was detected by Q-FISH assay through the flow cytometric method. Each experiment was repeated three times. *P<0.001 compared with the control.

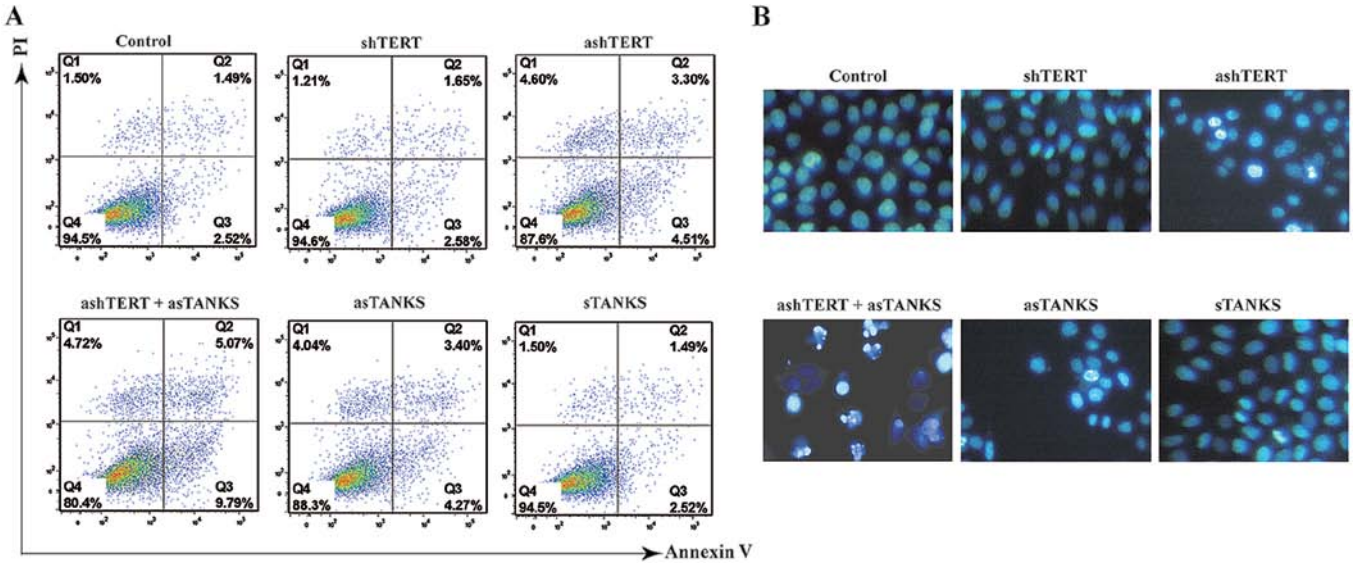

Figure 3. The apoptosis rate and nuclear morphology changes in A549 cells. (A) The apoptosis rate of A549 cells was detected by flow cytometry through Annexin V/PI double staining method; Q1 (Annexin V^-, PI^+) were dead cells, Q2 (Annexin V^+, PI^+) were late stage apoptosis cells, Q3 (Annexin V^+, PI^-) were early stage apoptosis cells, and Q4 (Annexin V^-, PI^-) were live cells. (B) The nuclear morphology changes were analyzed by fluorescence microscopy in x400 magnification using the Hoechst 33342 nuclear fluorescent dye staining. These experiments were performed 48 h after transfection.

centrifuged at 300 x g for 5 min at 20˚C and then washed with 10 ml RPMI-1640 complete medium twice. The labeled cells were the parent generation and the cultured cells were the daughter generation. Data are described as proliferation index (PI) analyzed by FlowJo (v7.6.5) software.

Tumor growth experiment in vivo. Female BALB/c nude mice were injected subcutaneously with $5x10^6$ A549 tumor cells transfected with or without oligonucleotide to the left flank. The length (L) and width (W) of tumors were measured regularly, and the volumes of tumor (V) were calculated by the following formula: $V = (L \times W^2)/2$.

Statistical analysis. Data are expressed as mean ± standard error of the mean and determined by ANOVA test. Differences were considered to be statistically significant when $P<0.05$.

Results

The corresponding antisense oligonucleotide decreases the expression of telomerase reverse transcriptase (TERT) and tankyrase. TERT, which is the telomerase catalytic subunit, is a ribonucleoprotein that synthesizes telomeric DNA repeats and keeps the length of telomere. In the present study, we transfected the ashTERT and asTANKS into A549 cells respectively or synchronously, at the same time corresponding shTERT and sTANKS were used as control. Our results showed that the expression of TERT and tankyrase decreased significantly after transfecting ashTERT or asTANKS 48 h later in both mRNA and protein level, but the corresponding sense control oligonucleotide showed no apparent change (Fig. 1). Of note, neither ashTERT nor asTANKS affected the expression to each other, while the combination of ashTERT and asTANKS

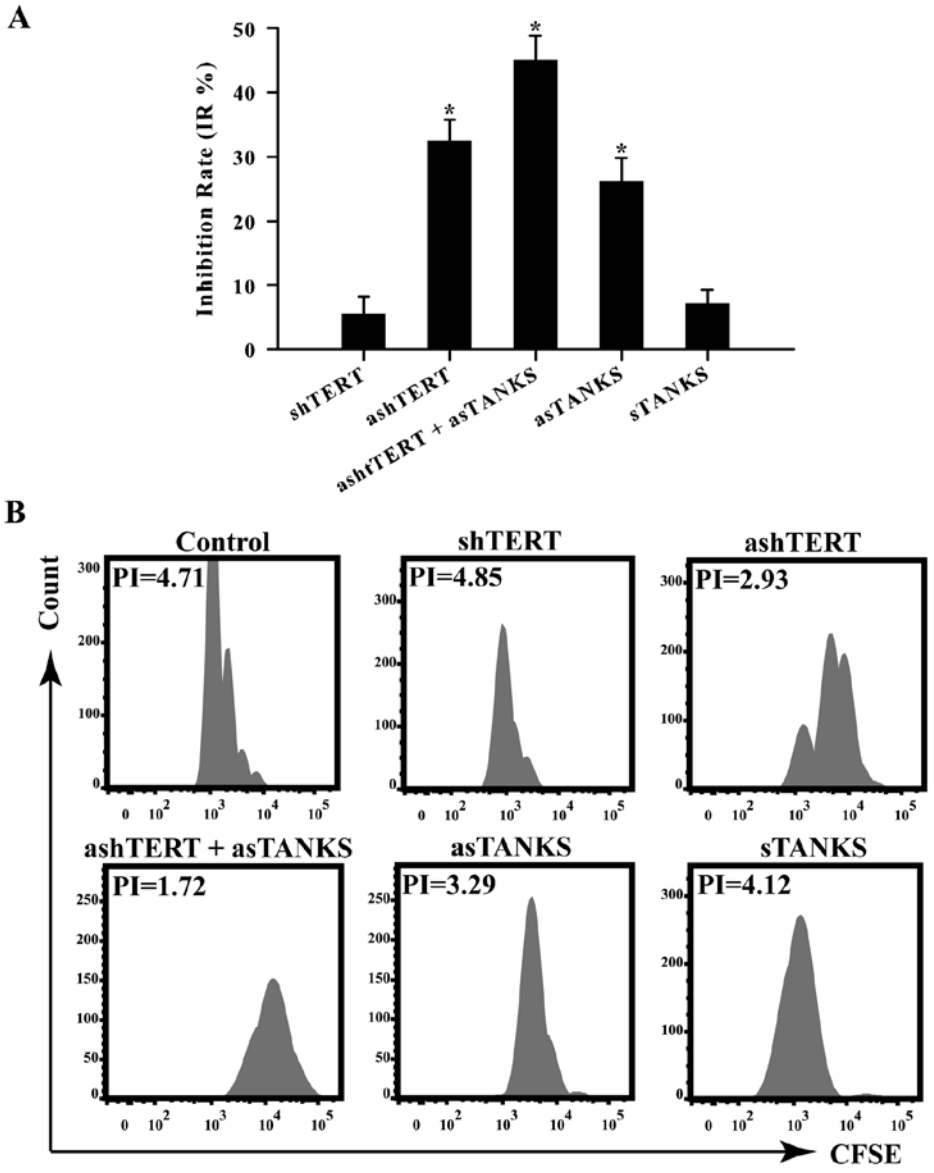

Figure 4. The proliferation capacity of A549 cells. (A) The proliferation inhibition rate caused by each oligonucleotide was detected by MTT assay and the absorbance at 490 nm was measured 48 h after transfection. The cell inhibition rate was calculated as % IR = (1 - $OD_{experiment}/OD_{control}$) x 100%; the data are shown as means ± SD. *P<0.05 compared with the control. (B) The cellular division capacity was tested by flow cytometry, A549 cells were stained by fluorescent dye CFSE, transfected by each oligonucleotide respectively and cultured another 48 h avoiding light; the mean fluorescence intensity of A549 cells was measured by flow cytometry and the PI was calculated by software FlowJo (v7.6.5).

downregulated TERT and tankyrase more efficiently than transfecting one of them alone (Fig. 1).

ashTERT and asTANKS reduce telomerase activity and shorten telomere length of A549 cells. Telomerase activity was decreased markedly by ashTERT and was uncorrelated with asTANKS (Fig. 2A). The related activity of telomerase in shTERT, ashTERT, ashTERT plus asTANKS, asTANKS and sTANKS group was 87.55±3.69, 37.75±2.79, 36.70±3.51, 81.14±4.65 and 83.44±4.13, respectively. There was a significant difference in telomerase activity between groups with and without ashTERT (P<0.001). However, regardless of asTANKS or sTANKS, telomerase activity was independent of them (P>0.05). The data supplied other evidence that the effect of tankyrase was unrelated to telomerase. Owing to different handling, there was statistical significance in mean telomere length, which corresponded to channel fluorescence intensity (FITC-labeled PNA probe) (Fig. 2B). With either asTANKS or ashTERT for 48 h, mean telomere length was 7.33±0.09, 7.59±0.07 kb, respectively, which was markedly lower than controls (P<0.001). However, regarding asTANKS or ashTERT, the combinated effect of both sides was more marked in shortening telomere length, in which mean telomere length was 3.55±0.08 kb (P<0.001).

ashTERT and asTANKS promote A549 cell apoptosis. In accordance with our hypothesis, ashTERT and asTANKS promoted A549 cell apoptosis. Furthermore, the ashTERT plus asTANKS group had the higher apoptosis percentage of all (Fig. 3A), the apoptosis rate (Q2 + Q3) in control, shTERT, ashTERT, ashTERT plus asTANKS, asTANKS and sTANKS group was 4.11±0.25, 4.23±0.21, 7.78±0.35, 14.87±0.42,

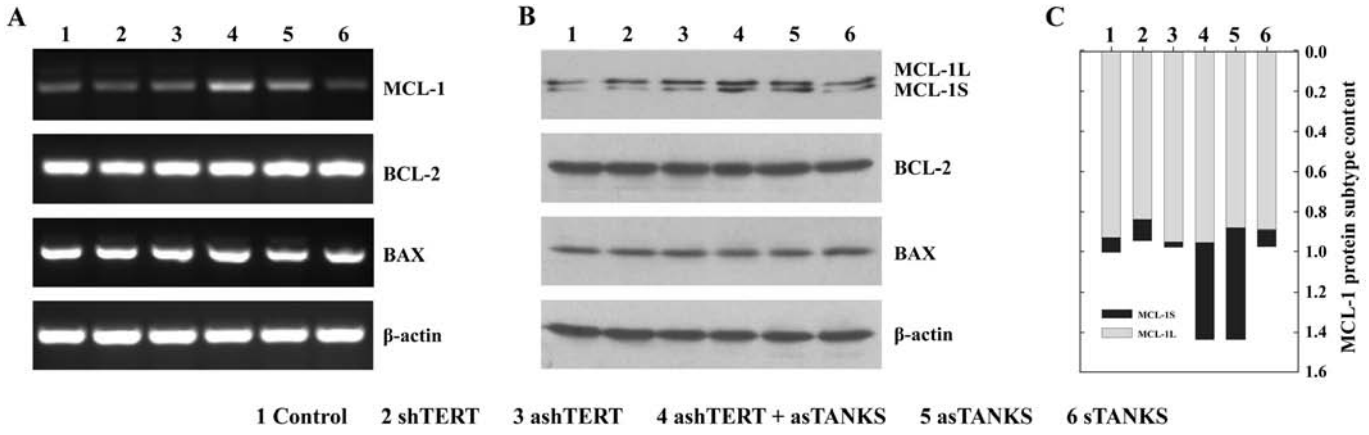

Figure 5. The expression of MCL-1, BCL-2, BAX and β-actin in A549 cells. A549 cells were transfected with ashTERT or asTANKS and the corresponding sense control oligonucleotide respectively; 48 h later, the expression of telomerase, tankyrase and β-actin were detected by (A) RT-PCR and (B) western blotting. (C) The western blot bands of MCL-1S and MCL-1L were analyzed by software ImageJ (v1.46r) and the relative content of these bands to the control were calculated.

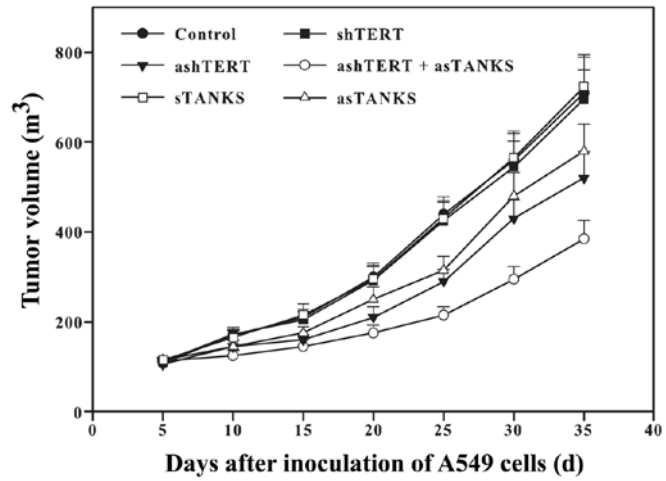

Figure 6. Tumor growth in nude mice. A549 cells were transfected with each oligonucleotide, respectively; 48 h later, $5x10^6$ A549 cells were inoculated in the left flank subcutaneously in the nude mice (n=6/group). Five days later, the length (L) and width (W) of tumors were measured with a microcaliper every five days until the 35th day, and the volumes of tumor (V) were calculated by the following formula: $V = (L \times W^2)/2$.

7.56±0.34 and 4.15±0.28%, respectively. Furthermore, we stained A549 cells with Hoechst 33342, a fluorescent dye that accumulated in apoptosis cells and showed that the dye increased in the ashTERT, asTANKS and ashTERT plus asTANKS groups, and, in particular, it clearly accumulated in the ashTERT plus asTANKS group (Fig. 3B).

ashTERT and asTANKS inhibit A549 cell proliferation. MTT proliferation assays were employed to further confirm the inhibitory effect on A549 cells caused by ashTERT and asTANKS. We measured absorbance at 490 nm and calculated inhibition rate as $IR = (1 - A490_{testing\ group}/A490_{control\ group}) \times 100\%$. Forty-eight hours after transfection, the absorbance at 490 nm was detected and the corresponding IR in shTERT, ashTERT, ashTERT plus asTANKS, asTANKS and sTANKS group was 5.51±2.76, 32.39±3.31, 45.06±3.73, 26.21±3.54, 7.07±2.23%; our findings showed that the ashTERT plus asTANKS group inhibited A549 cells proliferation the most efficiently (Fig. 4A). We labeled A549 cells with 5(6)-Carboxyfluorescein diacetate N-succinimidyl ester (CFSE), a fluorescent dye that can stain live cells and the fluorescence intensity detected by flow cytometry weakens followed by mitosis which was used to calculate PI by software FlowJo (v7.6.5). The PI in control, shTERT, ashTERT, ashTERT plus asTANKS, asTANKS and sTANKS group was 4.68±0.17, 4.82±0.20, 2.95±0.15, 1.70±0.12, 3.28±0.16, 4.21±0.23 (Fig. 4B). The results were consistent with the MTT assay that the asTANKS plus sTANKS group had the strongest ability to inhibit A549 cell proliferation.

asTANKS increases the expression of MCL-1 in A549 cells. ashTERT and asTANKS enhanced A549 cell apoptosis in the above study, and, thus, it is likely that some apoptosis-associated gene may have changed after transfecting by them. In order to confirm this hypothesis, the anti-apoptotic gene BCL-2, the pro-apoptotic gene BCL-2-associated X protein (BAX) and the bcl-2-like protein (MCL-1) were measured by RT-PCR (Fig. 5A) and western blotting (Fig. 5B). The results showed that neither ashTERT nor shTERT affected the expression of BCL-2, BAX and MCL-1 in mRNA and protein level in A549 cells, but asTANKS upregulated the MCL-1 mRNA markedly. The combination of asTANKS and ashTERT also led to a clear MCL-1 overexpression but it did not influence BCL-2 and BAX expression. Of note, MCL-1Short (MCL-1S), a pro-apoptotic short isoform, increased more than the alternatively spliced longer gene product MCL-1Long (MCL-1L) (Fig. 5B and C), which is an anti-apoptotic isoform. This may explain the molecular mechanism for asTANKS accelerating A549 cells apoptosis.

ashTERT and asTANKS inhibit A549 growth in vivo. The above results revealed that ashTERT and asTANKS promoted A549 cell apoptosis and inhibited their proliferation *in vitro*. In order to observe their effect *in vivo*, we inoculated A549 cells subcutaneously in the nude mice after transfection for 48 h. It showed that both ashTERT and asTANKS inhibited A549 cell proliferation and the tumor volume in the ashTERT plus asTANKS group was the least of all (Fig. 6).

Discussion

Telomerase and tankyrase play an important role in maintaining cell telomere length and cell division capacity. They are always at high levels in several types of malignant cancer, such as lung cancer (8), gastric cancer (9) and prostate cancer (10). Additionally, the higher their expression in cancer the poorer the prognosis in patients, therefore telomerase and tankyrase are gradually becoming targets of anticancer drugs.

Several telomerase and tankyrase inhibitors have been developed to treat cancer and present favorable antitumor effects, including azidothymidine (AZT), a telomerase inhibitor that can suppress reverse transcriptase activity of telomerase, promote apoptosis of human liver cancer cells HepG2 and SMMC-7721 and inhibit their proliferation (11). The tankyrase inhibitor JW55 which suppresses poly(ADP-ribose) polymerase (PARP) domain of tankyrase also suppressed SW480 human colon cancer cell proliferation by blocking the Wnt signaling pathway (12).

In the present study, ashTERT and asTANKS were used as the special inhibitors to silence the expression of target genes in human lung adenocarcinoma cells by transfection. At the same time, the corresponding sense oligonucleotides were used as control. Similar to the previously published reports, both ashTERT and asTANKS led A549 cells to apoptosis and suppressed proliferation. Moreover, combined ashTERT and asTANKS enhanced these effects; thus, the results indicated that asTANKS could improve the antitumor effect of ashTERT. In this report, it was also observed that ashTERT and asTANKS shortened the telomere length and, similarly, the combined group presented the more evident effect. Only ashTERT suppressed the telomerase reverse transcriptase activity, but asTANKS had almost no effect on it. Furthermore, asTANKS did not yet enhance this effect of ashTERT. Consistent with a previous study, the antisense oligonucleotide of tankyrase also shortened the length of telomere in SGC-7901 human gastric cancer cells and did not affect telomerase activity (13). Thus, it should be noted that asTANKS did not affect the telomerase activity directly, but it reduced the length of telomere in A549 cells by inhibiting the expression of tankyrase, leading to the telomere structure becoming tight and inhibiting telomerase approaching the telomere to elongate.

The telomere shortening can cause apoptosis of tumor cells (14). In the present study, we detected the cardinal anti-apoptotic gene BCL-2 and the pro-apoptotic gene BAX, but neither ashTERT nor asTANKS altered the expression of these genes. MCL-1, which can interact with tankyrase directly and regulate apoptosis, has two alternative splicing transcript variants which have distinct functions (15). MCL-1L is a long transcript variant that has been shown to form heterodimers with pro-apoptotic proteins BIM and BAK, and which suppresses the release of cytochrome *c* to inhibit apoptosis (16). MCL-1S combines with MCL-1L directly to promote apoptosis (17), thus the rate of these two isoforms determines the cell apoptosis. In this study, asTANKS upregulated the expression of MCL-1L and MCL-1S, and MCL-1S increased more significantly, ashTERT strengthened asTANKS effect but ashTERT alone had no such effect. Similarly, *in vivo* ashTERT and asTANKS suppressed the growth of A549 in nude mice and the A549 tumor grew the slowest in the combined group.

Telomere maintenance by telomerase is the key point of infinite growth for most cancer cells. Continuous treatment of cancer cells with telomerase inhibitors shortens telomeres and eventually induces cellular apoptosis. Moreover, there were 19 phase I, II or III clinical trials regarding telomerase inhibitor running in 2012 worldwide, and it may become the target of cancer therapy (18).

A potential disadvantage is that telomere shortening depends on the repetitive occurrence of the DNA end replication problem resulting from cell division (19). For this reason, it is essential that telomerase inhibitors are not cytotoxic. Furthermore, as telomere loss is a gradual process there is a lag between the time telomerase is inhibited and the time telomeres shorten sufficiently to disrupt the capping function. This would necessitate long treatment schedules that may lead to acquired drug resistance both in the cell and throughout the body. In general, longer telomeres provide more binding sites for TRF1, which blocks telomere access to telomerase. Accordingly, telomere shortening compromises the effect of telomerase inhibitors since shorter telomeres have fewer TRF1 molecules and therefore allow easier access to residual telomerase activity. Thus, the rate of telomere shortening per cell division decreases with telomere shortening itself. This phenomenon results from the incomplete shutdown of telomerase activity by telomerase inhibitors. A better therapeutic outcome may result from increasing the efficiency of telomere shortening to hasten the telomere crisis.

Telomere accessibility is also a potential target for telomerase inhibition. Inhibition of tankyrases, that enhance telomerase access to telomeres, may indirectly induce cancer cell senescence by abrogating telomerase activity (20). Tankyrase inhibitors enhance the rate of telomere shortening by means of a telomerase inhibitor, and induce earlier cell crisis. Tankyrase inhibitors do not directly inhibit telomerase activity but lead to telomere shortening, to a small extent, presumably by reducing telomere access to telomerase. Thus, it is expected that the effect of such tankyrase inhibitors on telomere length is selective to telomerase-positive cells and these provide support for tankyrase 1 as a suitable target for telomere-directed cancer therapy.

These observations suggest that the pharmacological targeting of tankyrase oligos is a potentially significant anticancer strategy if used in conjunction with telomerase inhibitors. This trend would further promote development not only of telomerase but also of tankyrase inhibitors.

Acknowledgements

The present study was supported by Grant 81101550 from the National Natural Science Foundation of China and the Natural Science Foundation of Hubei Province, China (no. 2012FFB05904).

References

1. Siegel R, Naishadham D and Jemal A: Cancer statistics, 2013. CA Cancer J Clin 63: 11-30, 2013.
2. Gadgeel SM, Ramalingam SS and Kalemkerian GP: Treatment of lung cancer. Radiol Clin North Am 50: 961-974, 2012.
3. Tümpel S and Rudolph KL: The role of telomere shortening in somatic stem cells and tissue aging: lessons from telomerase model systems. Ann NY Acad Sci 1266: 28-39, 2012.

4. Gomez DE, Armando RG, Farina HG, Menna PL, Cerrudo CS, Ghiringhelli PD and Alonso DF: Telomere structure and telomerase in health and disease (Review). Int J Oncol 41: 1561-1569, 2012.
5. Shay JW and Wright WE: Role of telomeres and telomerase in cancer. Semin Cancer Biol 21: 349-353, 2011.
6. Ruden M and Puri N: Novel anticancer therapeutics targeting telomerase. Cancer Treat Rev 39: 444-456, 2013.
7. Riffell JL, Lord CJ and Ashworth A: Tankyrase-targeted therapeutics: expanding opportunities in the PARP family. Nat Rev Drug Discov 11: 923-936, 2012.
8. Cha N, Li XY, Zhao YJ, Wang EH and Wu GP: hTERT gene amplification and clinical significance in pleural effusions of patients with lung cancer. Clin Lung Cancer 13: 494-499, 2012.
9. Gigek CO, Leal MF, Silva PN, Lisboa LC, Lima EM, Calcagno DQ, Assumpção PP, Burbano RR and Smith Mde A: hTERT methylation and expression in gastric cancer. Biomarkers 14: 630-636, 2009.
10. Bantis A, Patsouris E, Gonidi M, Kavantzas N, Tsipis A, Athanassiadou AM, Aggelonidou E and Athanassiadou P: Telomerase RNA expression and DNA ploidy as prognostic markers of prostate carcinomas. Tumori 95: 744-752, 2009.
11. Chen C, Zhang Y, Wang Y, Huang D, Xi Y and Qi Y: Synergic effect of 3'-azido-3'-deoxythymidine and arsenic trioxide in suppressing hepatoma cells. Anticancer Drugs 22: 435-443, 2011.
12. Waaler J, Machon O, Tumova L, Dinh H, Korinek V, Wilson SR, Paulsen JE, Pedersen NM, Eide TJ, Machonova O, Gradl D, Voronkov A, von Kries JP and Krauss S: A novel tankyrase inhibitor decreases canonical Wnt signaling in colon carcinoma cells and reduces tumor growth in conditional APC mutant mice. Cancer Res 72: 2822-2832, 2012.
13. Zhang H, Yang MH, Zhao JJ, Chen L, Yu ST, Tang XD, Fang DC and Yang SM: Inhibition of tankyrase 1 in human gastric cancer cells enhances telomere shortening by telomerase inhibitors. Oncol Rep 24: 1059-1065, 2010.
14. Zhang X, Mar V, Zhou W, Harrington L and Robinson MO: Telomere shortening and apoptosis in telomerase-inhibited human tumor cells. Genes Dev 13: 2388-2399, 1999.
15. Bae J, Donigian JR and Hsueh AJ: Tankyrase 1 interacts with Mcl-1 proteins and inhibits their regulation of apoptosis. J Biol Chem 278: 5195-5204, 2003.
16. Adams KW and Cooper GM: Rapid turnover of mcl-1 couples translation to cell survival and apoptosis. J Biol Chem 282: 6192-6200, 2007.
17. Bae J, Leo CP, Hsu SY and Hsueh AJ: MCL-1S, a splicing variant of the antiapoptotic BCL-2 family member MCL-1, encodes a proapoptotic protein possessing only the BH3 domain. J Biol Chem 275: 25255-25261, 2000.
18. Buseman CM, Wright WE and Shay JW: Is telomerase a viable target in cancer? Mutat Res 730: 90-97, 2012.
19. Tian X, Chen B and Liu X: Telomere and telomerase as targets for cancer therapy. Appl Biochem Biotechnol 160: 1460-1472, 2010.
20. Seimiya H: The telomeric PARP, tankyrases, as targets for cancer therapy. Br J Cancer 94: 341-345, 2006.